

# PERFORMANCE ANALYSIS OF SPACE SURVEILLANCE AND TRACKING SYSTEMS IN LEO

Arcos, A. <sup>(1)</sup> and Rueda, M. <sup>(2)</sup>

<sup>(1)</sup>University of Granada , 18013 Granada, Spain, Email: e.aarcos@go.ugr.es

<sup>(2)</sup>University of Granada , 18013 Granada, Spain, Email: mrueda@ugr.es

## ABSTRACT

Space Surveillance and Tracking (SST) is a progressively crucial research field due to the exponential growth of space debris. Along this paper several space environments will be reproduced while a space surveillance and tracking system is operating at LEO. Nowadays, there exist several ways of tracking & cataloguing space items, however, its exponential growth together with the bias and variance introduced by the surveillance systems, suppose a challenge in Orbit Determination and cataloguing of new objects.

In this work, state of art filtering and associating algorithms are implemented, optimized and compared in different space environments. To do so, debris, surveillance stations and the space medium are statistically modelled to generate synthetic data which, reliably represent LEO environment producing a highly-sampled analysis of the algorithms.

Finally, Multi-Target-Tracker (MTT) system is compared with classical error metrics such as Mean Square Error or Average Normalized-Estimation Error Squared and tracking-oriented metrics such as Optimal Sub-Pattern Assignment .

Keywords: LEO; Joint Probabilistic Data Association; Kalman; Filter; Track-Oriented Multi Hypothesis Tracker; Optimal Sub-Pattern Assignment; General Nearest Neighbour; Multi Target Tracker.

## 1. INTRODUCTION

Space Surveillance & Tracking is the field of study which detects, tracks, monitors and catalogues objects such as active/inactive satellites, spent rocket bodies, or fragmentation debris. However, the amount of them, its size and the distance to the tracking units block the detection of every human-made item in space. Attending to this, an SST MTT can be splitted into three main parts (Figure 2): initial orbit determination, statistical orbit determination and correlation. Each of them contains different algo-

rithms with its hyper-parameters that defines the performance of the system and so will be optimized with synthetic data created for different LEO scenarios.

### 1.1. Initial Orbit Determination (IOD)

IOD, as its noun refers, is the first calculation of the orbital parameters of a body moving in space. Since the first astronomers, IOD has been studied, as this first object state is fundamental for every astrodynamical problem as a state vector. Nonetheless, even for high-accuracy modern sensors it is a complex task due to the size and distance of space debris. During this work, as the measurement instruments modelled are basic mono-static radar sensors, they will only record position measurements in ECEF coordinates and time. Due to this restriction, the used IOD method for the system will depend on its mathematical nature. Gibbs, Herrick-Gibbs and Gauss will be preferred depending on the track length as per [21].

### 1.2. Statistical Orbit Determination (SOD)

Nowadays, space problems require of the highest possible precision to perform in line with the intrinsic uncertainties of space environment. This thought comes to correct the IOD of a body to actually determine its precise orbit, in which is known as Statistical Orbit Determination. Although it can be done with different approximations to the problem, state of the art [41], [37], [38] usually perform differential corrections of the orbital state using an estimation filter. In this framework, as one of the main parts affecting the tracker performance, most extended-used non-linear filters i.e. Extended Kalman Filter (EKF), Unscented Kalman Filter (UKF) and Particle Filter (PF), will be implemented as an tunable parameter of the MTT.

### 1.3. Correlation

A space surveillance system not only detects and predicts the orbital state of a space debris but also must be able to

Table 1. Space Surveillance Stations Location

	Location
St-1	10° N 180° E
St-2	0° N 20° W
St-3	65° N 20° W
St-4	90° S 0° E
St-5	35° N 136° E
St-6	51° N 7° E
St-7	30° S 71° W
St-8	70° N 20° E
St-9	30° N 86° W
St-10	7° S 72° E

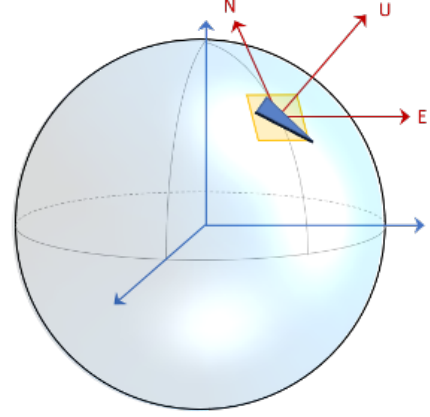


Figure 1. Ground Reference Frame

create, delete and update a space object catalogue. The main issue of correlating comes due to the limited number of radars and telescopes allowing only shots measurements (tracklets) as they cannot state a precise orbital state and so may be compared with objects in the catalogue, with other measurements or by IOD create a new object. This step, may seem straight forward, however due to the computational cost of the algorithms and the continuously growing object list is the most challenging topic in this field. Among SST, several algorithms and methods are used to match observations with tracklets exist, but they all could be classified in: Track-to-Orbit Correlation [31]& [12], Track-to-Track Correlation [39] & [19] and Orbit-to-Orbit Correlation [32]. The main part of this paper will be dedicated to these assignment algorithms in between three of them are remarked Global Nearest Neighbour (GNN), Joint Probabilistic Data Association (JPDA) & Multi-Hypothesis Tracker (MHT).

## 2. STATISTICAL SPACE MODELLING OF LEO

In order to test the performance of each algorithm, synthetic data should be created to faithfully represent the space environment. That implies creating a model to each one of the parts involved in the scenario: the sensor (stations), the mean (atmosphere and vacuum) and the target (debris). All these items are created in a virtual environment based on statistics.

### 2.1. Space Surveillance Stations

Space surveillance stations are complex facilities designed to increase the precisions of its devices measurements. However, in this paper, they will be simply modelled as an mono-static radar mounted on a 5 m platform and oriented to zenith as it can me seen on Figure 1. The location of these platforms are selected from real ESA-friendly stations [42] and resumed in Table 1.

**Mono-static Radar** A mono-static radar sensor is statistically modelled trough an algorithm to in each time step:

- Detects all targets within the Field of View (FoV): returns only emissions which fall within the receiver's bandwidth and where the receiver falls within the transmitter's FoV;
- Compute the Signal-to-Noise Ratio (SNR) for each target as:

$$SNR = RadarLoopGain + RCS - 40\log_{10}(r) \quad (1)$$

where,

$$RadarLoopGain = \frac{G_t A_r \sigma}{(4\pi)^2 r^4} \quad (2)$$

- Add losses from interfering emissions: Radar detection error is a random variable  $X_i: \Omega \rightarrow \mathbb{R}$  with  $E[X_i] = \mu < \infty$  and  $\text{var}[X_i] = \sigma^2 < \infty$ . A reduced variable is defined as  $\hat{X} = \frac{1}{n} \sum_{i=1}^n X_i$ . By Center Limit Theorem (CLT), as  $n \rightarrow \infty$ ,  $\hat{X} \rightarrow N(\mu, \sigma^2/n)$ ;

This study is focused on objects situated in LEO ranges, and so [13] recommend the parameter physical properties for a radar depicted in Table 2, which results on a statistical model with properties showed in Table 3

Table 2. Radar Parameters

FoV [deg]	El Res. [deg]	Range Res. [m]	Az Res. [deg]
[120 30]	0.01	100	0.01

### 2.2. Atmosphere & Vacuum

The radar algorithms introduce losses as stated in 2.1 in range and elevation due to the propagation of a wave

Table 3. Radar Model

Ref. Range [m]	False Alarm Prob. $P_{FA}$	Detection Prob. $P_D$
2000000	1e-6	0.9

through the troposphere using a single exponential model [11]. These phenomena is even more pronounced as the atmosphere is thicker, i.e. when the line-of-sight path between the radar and target lies at lower altitudes as per [10].

### 2.3. Debris

To model space debris motion, accounting for any kind of orbital state that lies in LEO a random orbit generator has been designed. A simplified perturbations model (SGP4) has been chosen to propagate the items in scenarios, assuming the Earth as a point mass body and negligible mass items. So in ECEF frame for a LEO:

$$\vec{a} = \frac{\mu}{r^3} \vec{r} - 2\Omega \times \frac{d}{dt} \vec{r} - \Omega \times (\Omega \times \vec{r}) + \vec{a}_{LEO}, \quad (3)$$

with,

$$\vec{a}_{LEO} = \vec{a}_{\odot} + \vec{a}_{\zeta} + \vec{a}_{SRP} + \vec{a}_{Drag} + \vec{a}_{NonSpherical}, \quad (4)$$

In order to introduce biases in the simulations, each one of the starting OE for each individual debris is randomized following Table 4.

Table 4. Randomized Debris Experiment

Orbital Element	Formula
Semi Major Axis (a) [m]	$7e6 + 1e5 \cdot P_a$
Eccentricity (e) [-]	$0.015 + 0.005 \cdot P_e$
Inclination (i) [deg]	$80 + 10 \cdot P_i$
Long. of Ascending Node ( $\Omega$ ) [deg]	$360 \cdot P_{\Omega}$
Argument of Periapsis ( $\omega$ ) [deg]	$360 \cdot P_{\omega}$
True Anomaly ( $\nu$ ) [deg]	$360 \cdot P_{\nu}$

where  $P_n$  is a randomized number between 0 and 1. Besides, each scenario is run 100 times and cross-validated [1] not to overhit the hyper-parameter optimization results.

### 2.4. Track Determination and Association

As any kind of autonomous system, tracking is an essential part for SST. A simple tracking system estimates the states of the target and their number based on kinematic observations and measurements along time and there is no need of association. However, real environments includes cluttering, biases, errors, etc, so that the received

measurements may not arise from a real object, and so Multiple Target Trackers are needed.

As it can be seen in 2, a MTT can be splitted into several systems: maintenance, filtering, gating and assignment.

#### 2.4.1. Maintenance

As was mentioned before, this kind of systems shall maintain a list of tracks generated to reduce the computational and memory cost of the system providing the filter with optimal tracks. Once a MTT is served with a tracklet it chooses whether initialise, confirm or delete tracks from the catalogue; that choice is made based on *Track Logic*. There exist two main philosophies in current literature:

- History-Based: in this logic, a thresholds is fixed as *M-out-of-N* ([M N]) then the algorithm polls the amount of measurements assigned to a track within several updates. If the number of detections is grater/lower than the established threshold, the track is confirmed/deleted.
- Score-Based [2]: in this case, the log-likelihood for each track to be a real target is calculated and confirmed or deleted based on a preset choice probability.

This part of the system acts as link between the catalogue and the surveillance stations, however, logics do not actuate in case of no already similar track maintained; in which the algorithm creates a new one; or no detections are assigned to a track, in which it coasted the track until next detection.

#### 2.4.2. Gating

In order to follow the multiple tracks created, a crucial part is whether to assign detections (x in Figure 3) to targets ( $T_n$  in Figure 3) or maintained tracks in order to amend them. As part of a large population this algorithm gets sophisticated with amount of detections, sensors resolution, probability of detection and false alarm rates.

As the computational performance is a need for large populations, gating is merged to the system in order to reduce the number of associations computed by the MTT, pruning the measurements that lands outside of the region defined by these gates. Due to the nature of the problem, elliptical gating will be used [40] based on a modified Mahalanobis-norm:

$$d_m = \Delta p S \Delta p^T + \log(|S|), \quad (5)$$

In which the first term attends for the distance between a point and a distribution and a second term is added to

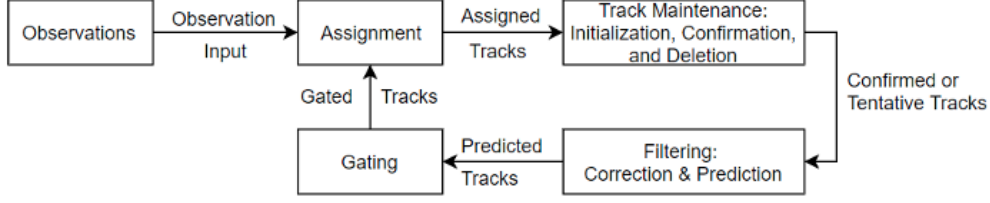


Figure 2. MTT Architecture

harm highly uncertain distribution. So the probability to accept correct measurement in the gate becomes:

$$P_G = \int_0^{\gamma_g} \chi^2(\gamma, 3) d\gamma, \quad (6)$$

in which the gate  $\gamma_g$  is the squares' sum of  $n$   $N(0, S_T)$  distributed variables is a  $\chi^2(n)$  distributed with  $n$  degrees of freedom.

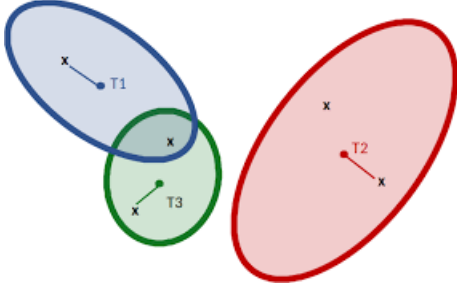


Figure 3. Gating Example [18]

Applying the mathematical methods explained above in the system will accept detections with a probability of 0.9 (matching 2.1) would be selected, creating a gate with  $\gamma_g \approx 10$  km.

#### 2.4.3. Filtering

Kalman filters are extensively used in tracking environments to estimate the state of an object in movement while measuring it [35],[16],[6]. These filters are recursive methods in which both the process and measurements have additive noises and that improve the prediction of target's state with each measurement. Also in this work an alternative to Kalman filters is studied: the particle filter (PF).

**Extended Kalman Filter (EKF)** Simplifying it if a noisy observation  $x_k$ , a recursive estimation for  $y_k$  can be expressed as [24]:

$$\hat{y}_k = \text{prediction of } y_k + K_k \cdot [x_k - (\text{prediction of } x_k)], \quad (7)$$

returning the optimal MSE for  $x_k$  assuming its previous step  $x_{k-1}$  and the observation  $y_k$  are Gaussian random variables [43].

An EKF is based on the following process: if a random variable  $x$  has mean  $\hat{x}$  and covariance  $Q_x$  and a nonlinear function of it  $y = g(x)$  has covariance  $R_y$ , the EKF is initialized as:

$$\hat{x}_0 = E[x_0], \quad (8)$$

$$P_0 = E[(x_0 - \hat{x}_0)(x_0 - \hat{x}_0)^T], \quad (9)$$

then foreseen dynamic state of  $x$  at a given time  $k$  given the measurements up to  $k-1$  and its covariance is:

$$\hat{x}_{k|k-1} = f(\hat{x}_{k-1|k-1}, u_k), \quad (10)$$

$$P_{k|k-1} = F_k P_{x,k-1|k-1} F_k^T + Q_x, \quad (11)$$

$$F_k = \frac{\partial f}{\partial x} \Big|_{\hat{x}_{k-1|k-1}, u_k}, \quad (12)$$

So, the measurement updated equations are given by:

$$\hat{y}_k = y_k - h(\hat{x}_{k|k}), \quad (13)$$

$$P_{y,k} = H_k P_{k|k-1} H_k^T + R_y, \hat{x}_{k|k} = \hat{x}_{k|k-1} + P_{k|k-1} H_k^T P_{y,k}^{-1} \hat{y}_k, \quad (14)$$

$$P_{k|k} = (I - P_{k|k-1} H_k^T P_{y,k}^{-1} H_k) P_{k|k-1}, \quad (15)$$

$$H_k = \frac{\partial g}{\partial x} \Big|_{\hat{x}_{k|k-1}, u_k}, \quad (16)$$

Even though this is explained for a first order EKF, the complexity of the filter gets higher by retaining more terms at the Taylor series expansion, which will be used for large noise detections (based on the SNR) as in [15].

**Particle Filter (PF)** The essential characteristic of these filters is to use a batch of particles around the current state to represent the posterior distribution of some random process. Due to its essence the assessment these filters are flexible and computationally expensive, underperforming in highly dimensional spaces [7] [9] [8].

Just as most filters, the most common applications of PF is system tracking [28] [22] [26] to sequentially estimate the future density of the state vector with Monte Carlo principles and Approximate Bayesian Computation techniques. Due to the complexity of the method, the algorithms is not presented but it can be found at [14].

**Unscented Kalman Filter (UKF)** Due to the estimation problems that other nonlinear KF had the UKF emerges coasting the dynamic state through a Gaussian random variable propagated by an unscented transformation such as in [20]; allowing a transformation of the state and its covariance that avoids first order linearisation of a nonlinear system.

The basis of this conversion is to estimate the mean state and its covariance spreading weighted sigma points around the mean state [43]. Although it can be seen as Monte Carlo method, UKFs perform significantly better than the rest of sampling methods offering even better accuracy [25].

Assuming that a random variable  $x$  has mean  $\hat{x}$  and covariance  $P_x$ :

$$\hat{x}_0 = E[x_0], \quad (17)$$

$$P_0 = E[(x_0 - \hat{x}_0)(x_0 - \hat{x}_0)^T], \quad (18)$$

$$\hat{x}_0^a = E[x_0^a] = [\hat{x}_0^T \ 0 \ 0]^T, \quad (19)$$

$$P_0^a = E[(x_0^a - \hat{x}_0^a)(x_0^a - \hat{x}_0^a)^T], \quad (20)$$

where the superscript  $a$  denotes for the original measurements and the sigma points for  $k \in [1, \dots, \infty]$  are calculated as:

$$X_{k-1}^a = [\hat{x}_{k-1}^a \pm \sqrt{(L + \lambda)P_{k-1}^a}], \quad (21)$$

being  $\lambda$  a composite scaling parameter and  $L$  the dimension of augmented state, with each time update:

$$X_{k|k-1}^x = F[X_{k-1}^x, X_{k-1}^v], \quad (22)$$

$$\hat{x}_k^- = \sum_{i=0}^{2L} W_i^{(m)} X_{i,k|k-1}^x, \quad (23)$$

$$P_k^- = \sum_{i=0}^{2L} W_i^{(c)} [X_{i,k|k-1}^x - \hat{x}_k^-][X_{i,k|k-1}^x - \hat{x}_k^-]^T, \quad (24)$$

$$Y_{k|k-1}^x = H[X_{k|k-1}^x, X_{k-1}^n], \quad (25)$$

$$\hat{y}_k^- = \sum_{i=0}^{2L} W_i^{(m)} Y_{i,k|k-1}^x, \quad (26)$$

$$(27)$$

where  $W_i$  is the weight of each sigma point. So, the measurement updated equations are:

$$P_{yy} = \sum_{i=0}^{2L} W_i^{(c)} [Y_{i,k|k-1} - \hat{y}_k^-][Y_{i,k|k-1} - \hat{y}_k^-]^T, \quad (28)$$

$$P_{xy} = \sum_{i=0}^{2L} W_i^{(c)} [X_{i,k|k-1} - \hat{x}_k^-][Y_{i,k|k-1} - \hat{y}_k^-]^T, \quad (29)$$

$$K = P_{xy}P_{yy}^{-1}, \quad (30)$$

$$\hat{x}_k = \hat{x}_k^- + K(y_k - \hat{y}_k^-), \quad (31)$$

$$P_k = P_k^- - KP_{yy}K^T, \quad (32)$$

System efficiency is the most relevant parameter for space surveillance meaning that the selection of best assignment algorithm is a key parameter to built a MTT. In this paper three of the most relevant ones will be compared [27].

**Global Nearest Neighbour (GNN)** The main idea of GNN algorithms is identify the best association for a detection-track couple to prune all other options. By doing so, the exact next density probability is approached by the chance of optimal association  $p_{k|k}(X_k) = p_{k|k}^{h_{opt,k}}(X_k)$ . Due to its simplicity, GNN algorithms ensure high computational efficiency while underperform in densely distributed spaces [23].

GNN is a data association approach which attempts to discover and propagate the most feasible candidates' tracks. The estimation of all tracks is accomplished by the likelihood theory, reducing a chosen metric. In this project the Mahalanobis distances to the measurement was chosen, however, GNN methods can also consider other metrics as shape, size, velocity or a combination of them.

**Joint Probabilistic Data Association (JPDA)** Trackers based on Joint Probabilistic Data Association (JPDA) assess the error covariance matrix and its state vector associated for each one of the items in catalogue. To do so. the algorithm apply a soft allocation when multiple measurements commit to each track. Although it can be based on different logics, the employed JPDA performs the weight sum (probabilistically determined) of all measurements in the gate, averaging over detections with related probabilities.

The main goal of JPDA is merging all marginal posterior densities to calculate the marginal correlation probabilities for all targets [17]. The evaluation of each joint likelihood at a given time is [3]:

$$p_{k|k}^{h_k}(x_k) = \prod_{j=1}^m g_{ij} P_D \cdot \prod_{j=1}^m (1 - P_D) \cdot \prod_{j=1}^m \beta, \quad (33)$$

where  $P_D$  is the detection likelihood,  $g_{ij}$  is the probability of observe  $j$  given the track  $i$  and  $\beta$  is the false alarm odds. The first term represents the chance of assigning the track  $i$  to the measurement  $j$ , the second indicates tracks assigned to no match while the last accounts for unassigned observations. Then, the probability of observation  $i$  to be assigned to the track  $j$  is:

$$p_{ij} = \sum_{h=1}^N p_{k|k}^{h_k}(x_k), \quad (34)$$

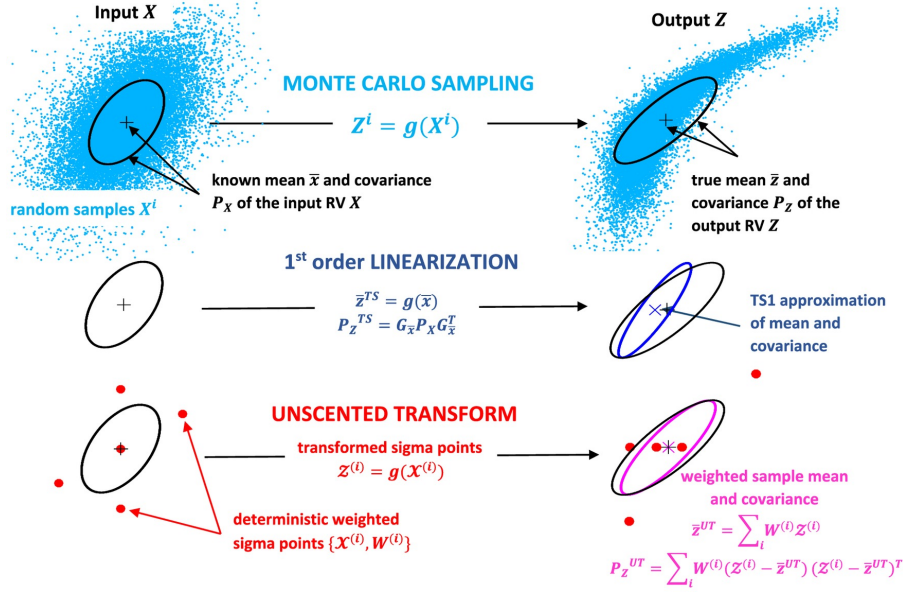


Figure 4. PF, EKF and UKF Principles [29]

**Track-Oriented Multiple Hypothesis Tracker (TOMHT)** Multiple Hypothesis algorithms evaluate the probability of all the association hypotheses considering the association of measurements' sequences. As in JPA, TOMHT calculates the probability of each association as in (33) but in this case it would expand each scenario independently, increasing the association accuracy.

Its basic idea [34] is, in each update, to find the best assignments and prune all others, reducing them such that a maximum number of hypotheses are included in the posterior density. A primitive TOMHT is parametrized by global hypotheses  $H_k$ , log-weights  $l^{h_k}$ , which are the natural logarithm of the probability from hypothesis  $h_k$ ; and the local hypotheses from each object  $p_{k|k}^{i,h_k}(x_k^i)$ .

TOMHT is designed to delay difficult data association to future data income. Besides the complexity of these approaches require a challenging system of tracking maintenance, filtering and mitigation strategies. TOMHT shows better performances than JPDA or GNN via higher computational cost and a complex implementation.

## 2.5. Tracking Metrics

SOD predict the states for targets, which continuously appear, move and disappear. The necessity of comparing and analysing the performance of these algorithms requires the usage of a new metric to compute the affinity betwixt truth state of the estimated tracks and synthetic data.

Contributions of [36] *Optimal SubPattern Assignment* and [33] *Generalized Optimal SubPattern Assignment*

would not only evaluate the performance of the orbit determination part but also analyse the efficiency of the correlation algorithms.

**Optimal SubPattern Assignment (OSPA)** OSPA can be define as:

$$OSPA(X, Y) = \frac{1}{|Y|} \left( \min \sum_{i=1}^{|X|} d^c(x_i, y_{\pi(i)})^p + c^p (|Y| - |X|)^{\frac{1}{p}} \right)^{\frac{1}{p}}, \quad (35)$$

in which several errors are considered:

- Localisation error is measured as the distance between  $x$  and  $y$  vectors, using the Mahalanobis modified distance [5].
- Assignment error chosen is the Auction proposed by [4] although, as with localisation, this function is customizable.

**Generalized Optimal SubPattern Assignment (GOSPA)** OSPA metric allows the tracker to have as false or missed detections as it wants, so the creation of a different penalisation for accurate, misplaced and erroneous detections lead to GOSPA. Similarly to its precursor:

$$GOSPA(X, Y) = \left( \min \sum_{i=1}^{|X|} d^c(x_i, y_{\pi(i)})^p + \frac{c^p}{\alpha} (|Y| - |X|)^{\frac{1}{p}} \right)^{\frac{1}{p}}, \quad (36)$$

where  $\alpha$  illustrates the Gaussian distribution similarity. GOSPA differs from OSPA in the  $\alpha$  parameter and is not normalized.

This metric encourage the system to improve their assignment performance over its state's precision so either OSPA or GOSPA could be chosen according to the tracker goals. In this case, at each step the metric aims assignment based on both the previous and current assignment metrics allowing the metric to easily record track events.

### 3. RESULTS

Table 5. IOD Method Errors

	posRMSE [m]	velRMSE [m/s]
Gibbs	-	67.7089
Gauss	-	69.28
Herrick-Gibbs	-	73.93

The simulation generating synthetic data is executed for a sidereal day in three different scenarios:

- 1<sup>st</sup> scenario is consisting the simplest case with just four stations and simplified debris dynamics and population (100). This scenario is used in order to quickly configure the best approach for the filter selection and the main hyper-parameters of the algorithms involved.
- 2<sup>nd</sup> scenario is build in a realistic LEO environment (as explained in previous sections) increasing the coverage and the complexity of the dynamics. In this scenario a fine hyper-parameter tuning [30] is perform to observe the dependence of this calibration on the scenarios.
- 3<sup>rd</sup> scenario increases the number of object to be tracked up to 10000 particles to be detected and catalogued. In this case, the 2<sup>nd</sup> scenario calibration is used.

Results and trade-off analyses converge to a common MTT configuration showed in Table 6.

Table 6. MTT System Optimal Configuration

Gating	Maintenance	Filter	Tracker
1e2 km	[7 10] & [2 3]	UKF	JPDA

The 2<sup>nd</sup> scenario optimal parameters are shown in Tables 7 and 8 while the results of the experiments are resumed in Tables 9 10, 11 and 12.

Table 7. Filters' Parameters

	EKF	PF	KF
$\sigma_{n_{pos}}$ [m]	0.4	0.4	0.4
$\sigma_{n_{vel}}$ [m/s]	0.4	0.4	0.4
$\sigma_{0_{pos}}$ [m]	1e3	1e3	1e3
$\sigma_{0_{vel}}$ [m/s]	1e4	1e4	1e4
State Estimation Method	-	Max Weight	-
Number of Particles	-	1e4	-

Table 8. Tracker Parameters

	GNN	JPDA	TOMHT
Confirmation Threshold	[7 10]	[7 10]	70
Deletion Threshold	[2 3]	[2 3]	-7
$\beta$ [ $1/m^3 s$ ]	5e-3	-	5e-3
Bin Volume [ $m^3$ ]	1.2337e+13	1.2337e+13	1.2337e+13
Clutter Density [ $1/m^3$ ]	-	8.1e-20	-

### 4. DISCUSSION

From results shown in previous section, several conclusions could be extracted:

- Probabilistic data association (JPDA & TOMHT) performs better overall, and this performance is maintained as the scenarios get complex, maintaining good accuracy and robustness metrics. Besides, JPDA maintain minimum impact on computing load compared to TOMHT, although in simple cases is really powerful, it underperforms in highly dimensional problems.
- UKF emerge as the best performing algorithm for filtering in the studied cases. However, PF performance could be more flexible as it is highly dependant on its hyper-parameters.
- The necessity of stating new metrics such as OSPA or GOSPA to include gating, maintaining and assignment algorithms on the SST system performance analysis. This is driven by the ambiguous relation of accuracy metrics and the non filter algorithms and the exponential growth of debris population.
- Optimizing MTT hyper-parameters enable large improvements on all its parts even for simple adjustments, reducing also the computational load on the system. Besides, using real sensor and surveillance data could greatly benefit this optimization processes continuously improving an already deployed surveillance station.

- Statistical simulation of the SST scenario could be extensively useful in design phases of the system, as it enables an estimation of the final accuracy results in early-phases of the project, allowing to optimize the system as a whole prior to its implementation.

As a conclusion, it could be seen how SST systems performance is a complex and high dimensional system, which is sensible to a wide range of parameters. System optimization enhances the possibilities of surveillance, however metrics to do so need to be carefully chosen, to not only include accuracy of the prediction but also considering the sensitivity, specificity and precision.

## REFERENCES

1. Anguita, D., Ghelardoni, L., Ghio, A., Oneto, L., and Ridella, S. (2012). The ‘k’ in k-fold cross validation. In *20th European Symposium on Artificial Neural Networks, Computational Intelligence and Machine Learning (ESANN)*, pages 441–446. i6doc. com publ.
2. Bar-Shalom, Y., Blackman, S. S., and Fitzgerald, R. J. (2007). Dimensionless score function for multiple hypothesis tracking. *IEEE Transactions on Aerospace and Electronic Systems*, 43(1):392–400.
3. Bar-Shalom, Y. and Li, X.-R. (1995). *Multitarget-multisensor tracking: principles and techniques*, volume 19. YBs Storrs, CT.
4. Bertsekas, D. P. (1979). A distributed algorithm for the assignment problem. *Lab. for Information and Decision Systems Working Paper, MIT*.
5. Blanco, J.-L., González-Jiménez, J., and Fernández-Madrigal, J.-A. (2012). An alternative to the mahalanobis distance for determining optimal correspondences in data association. *IEEE transactions on robotics*, 28(4):980–986.
6. Chan, Y., Hu, A., and Plant, J. (1979). A kalman filter based tracking scheme with input estimation. *IEEE transactions on Aerospace and Electronic Systems*, AES-15(2):237–244.
7. Del Moral, P. (1997). Nonlinear filtering: Interacting particle resolution. *Comptes Rendus de l’Académie des Sciences-Series I-Mathematics*, 325(6):653–658.
8. Del Moral, P. and Doucet, A. (2003). On a class of genealogical and interacting metropolis models. In *Séminaire de Probabilités XXXVII*, pages 415–446. Springer.
9. Del Moral, P. et al. (1998). Measure-valued processes and interacting particle systems. application to nonlinear filtering problems. *The Annals of Applied Probability*, 8(2):438–495.
10. Doerry, A. W. (2013a). Earth curvature and atmospheric refraction effects on radar signal propagation. *Sandia Report SAND2012-10690*.
11. Doerry, A. W. (2013b). Radar range measurements in the atmosphere. *Sandia Report SAND2013-1096, Unlimited Release*.
12. Domínguez-González, R., Sánchez-Ortiz, N., Guijarro-López, N., Quiles-Ibernón, P., and Nomen-Torres, J. (2017). Cataloguing space objects from observations: Corto cataloguing system. In *7th European Conference on Space Debris*.
13. Donath, T., Michal, T., Vanwijck, X., Dugrosprez, B., Menelle, M., Flohrer, T., Schildknecht, T., Martinot, V., Leveau, J., Ameline, P., et al. (2005). Detailed assessment of a european space surveillance system. *Final report to ESA study*, 18574(04).
14. Doucet, A. and Johansen, A. M. (2009). A tutorial on particle filtering and smoothing: Fifteen years later. *Handbook of nonlinear filtering*, 12(656-704):3.
15. Einicke, G. A. (2019). Smoothing, filtering and prediction: Estimating the past, present and future second edition.
16. Farahi, F. and Yazdi, H. S. (2020). Probabilistic kalman filter for moving object tracking. *Signal Processing: Image Communication*, 82:115751.
17. Fortmann, T., Bar-Shalom, Y., and Scheffe, M. (1983). Sonar tracking of multiple targets using joint probabilistic data association. *IEEE journal of Oceanic Engineering*, 8(3):173–184.
18. Hendeby, G. and Karlsson, G. (2019). Target tracking.
19. Hill, K., Sabol, C., and Alfriend, K. T. (2012). Comparison of covariance based track association approaches using simulated radar data. *The Journal of the Astronautical Sciences*, 59(1-2):281–300.
20. Julier, S. J. and Uhlmann, J. K. (1997). New extension of the kalman filter to nonlinear systems. In *Signal processing, sensor fusion, and target recognition VI*, volume 3068, pages 182–193. International Society for Optics and Photonics.
21. Kaushik, A. S. (2016). *A Statistical Comparison Between Gibbs and Herrick-Gibbs Orbit Determination Methods*. PhD thesis, Texas A & M University.
22. Khan, Z., Balch, T., and Dellaert, F. (2005). Mcmc-based particle filtering for tracking a variable number of interacting targets. *IEEE transactions on pattern analysis and machine intelligence*, 27(11):1805–1819.
23. Konstantinova, P., Udvarev, A., and Semerdjiev, T. (2003). A study of a target tracking algorithm using global nearest neighbor approach. In *Proceedings of the International Conference on Computer Systems and Technologies (CompSysTech’03)*, pages 290–295.
24. Lewis, F. L. (1986). *Optimal estimation, a wiley-interscience publication*.
25. Manish, R. (2014). Linear and non-linear estimation techniques: Theory and comparison. *arXiv preprint arXiv:1406.5556*.
26. Mashiku, A., Garrison, J., and Carpenter, J. R. (2012). Statistical orbit determination using the particle filter for incorporating non-gaussian uncertainties. In *AIAA/AAS Astrodynamics Specialist Conference*, page 5063.



27. McMillan, J. C. and Lim, S. S. (1990). Data association algorithms for multiple target tracking. Technical report, DEFENCE RESEARCH ESTABLISHMENT OTTAWA (ONTARIO).
28. Okuma, K., Taleghani, A., De Freitas, N., Little, J. J., and Lowe, D. G. (2004). A boosted particle filter: Multitarget detection and tracking. In *European conference on computer vision*, pages 28–39. Springer.
29. Olivier, A. and Smyth, A. W. (2017). Review of nonlinear filtering for shm with an exploration of novel higher-order kalman filtering algorithms for uncertainty quantification. *Journal of Engineering Mechanics*, 143(11):04017128.
30. Ozaki, Y., Tanigaki, Y., Watanabe, S., and Onishi, M. (2020). Multiobjective tree-structured parzen estimator for computationally expensive optimization problems. In *Proceedings of the 2020 genetic and evolutionary computation conference*, pages 533–541.
31. Pastor, A., Escobar, D., Sanjurjo, M., and Águeda, A. (2019). Data processing methods for catalogue build-up and maintenance. In *1st NEO and Debris Detection Conference*.
32. Pastor-Rodríguez, A., Escobar, D., Sanjurjo-Rivo, M., and Águeda, A. (2018). Correlation techniques to build-up and maintain space objects catalogues. In *Proceedings of the 7th International Conference on Astrodynamics Tools and Techniques (ICATT)*, pages 6–9.
33. Rahmathullah, A. S., García-Fernández, Á. F., and Svensson, L. (2017). Generalized optimal sub-pattern assignment metric. In *2017 20th International Conference on Information Fusion (Fusion)*, pages 1–8. IEEE.
34. Reid, D. (1979). An algorithm for tracking multiple targets. *IEEE transactions on Automatic Control*, 24(6):843–854.
35. Roy, A. and Mitra, D. (2016). Unscented-kalman-filter-based multitarget tracking algorithms for airborne surveillance application. *Journal of Guidance, Control, and Dynamics*, 39(9):1949–1966.
36. Schuhmacher, D., Vo, B.-T., and Vo, B.-N. (2008). A consistent metric for performance evaluation of multi-object filters. *IEEE transactions on signal processing*, 56(8):3447–3457.
37. Schutz, B., Tapley, B., and Born, G. H. (2004). *Statistical orbit determination*. Elsevier.
38. Shi, C., Zhao, Q., Li, M., Tang, W., Hu, Z., Lou, Y., Zhang, H., Niu, X., and Liu, J. (2012). Precise orbit determination of beidou satellites with precise positioning. *Science China Earth Sciences*, 55(7):1079–1086.
39. Siminski, J. (2016). Techniques for assessing space object cataloguing performance during design of surveillance systems. In *6th International Conference on Astrodynamics Tools and Techniques (ICATT)*, pages 14–17.
40. Singh, S. K., Premalatha, M., and Nair, G. (1995). Ellipsoidal gating for an airborne track while scan radar. In *Proceedings International Radar Conference*, pages 334–339. IEEE.
41. Tapley, B. D. (1973). Statistical orbit determination theory. In *Recent Advances in Dynamical Astronomy*, pages 396–425. Springer.
42. Vallado, D. A. and Griesbach, J. D. (2011). Simulating space surveillance networks. In *Paper AAS 11-580 presented at the AAS/AIAA Astrodynamics Specialist Conference*. July.
43. Wan, E. A. and Van Der Merwe, R. (2000). The unscented kalman filter for nonlinear estimation. In *Proceedings of the IEEE 2000 Adaptive Systems for Signal Processing, Communications, and Control Symposium (Cat. No. 00EX373)*, pages 153–158. Ieee.

Table 9. Tracker Results 1<sup>st</sup> Scenario

	JPDA		GNN		TOMHT	
	$\mu$	$\sigma$	$\mu$	$\sigma$	$\mu$	$\sigma$
posRMSE [m]	1519.0551	575.79394	203385.4468	332114.832	20653.5197	72153.1144
velRMSE [m/s]	2.5156	0.666	382.0123	598.4253	110.2248	653.4519
posANEES [-]	3.5746	6.5206	53497.428984	1664481.2314	1.0091	1.9903
velANEES [-]	0.69903	1.0341	8847.60577	21674.1117	0.31866	0.58786
OSPA [-]	2.4702	1.2965	8.8321	1.5266	<b>1.4415</b>	1.0077
GOSPA [-]	95.2694	60.7968	1.1267e+06	3.7174e+07	<b>64.0749</b>	18.4566
Time [s]	10369.9707		6979.8365		6705.0962	

Table 10. Filter Results 1<sup>st</sup> Scenario

	EKF		PF		UKF	
	$\mu$	$\sigma$	$\mu$	$\sigma$	$\mu$	$\sigma$
posRMSE [m]	4601.3034	1778.1254	1828.2889	678.60118	1519.0551	575.79394
velRMSE [m/s]	7.6973	1.9103	3.6761	9.3951	2.5156	0.666
posANEES [-]	7.5984	5.63	2.6179	5.1537	3.5746	6.5206
velANEES [-]	4.032	8.2594	0.94851	4.7608	0.69903	1.0341
OSPA [-]	5.1457	1.6035	<b>2.4985</b>	1.0221	<b>2.4702</b>	1.2965
GOSPA [-]	116.4202	48.62607	<b>83.0267</b>	134.4164	<b>95.2694</b>	60.7968
Time [s]	12234.908		11992.7309		10369.9707	

Table 11. Tracker Results 2<sup>nd</sup> Scenario

	JPDA		GNN		TOMHT	
	$\mu$	$\sigma$	$\mu$	$\sigma$	$\mu$	$\sigma$
posRMSE [m]	1737.3771	665.6931	2399.6865	914.94592	2438.8459	1116.8946
velRMSE [m/s]	2.9205	0.71529	4.3666	1.5296	4.9623	3.9535
posANEES [-]	2.1991	3.4179	3.1995	3.2784	2.4403	2.0419
velANEES [-]	0.62031	0.81893	1.3362	1.9018	0.88658	0.73338
OSPA [-]	<b>2.3488</b>	1.0911	3.1238	1.0632	<b>3.1733</b>	1.0689
GOSPA [-]	<b>74.6093</b>	27.516	81.3418	33.1463	<b>70.6277</b>	13.5744
Time [s]	11589.8886		14719.626		14177.4883	

Table 12. Tracker Results 3<sup>rd</sup> Scenario

	JPDA		GNN		TOMHT	
	$\mu$	$\sigma$	$\mu$	$\sigma$	$\mu$	$\sigma$
posRMSE [m]	2275.7237	768.99155	501525.3396	269378.9326	2530.8173	645.14598
velRMSE [m/s]	3.9362	2.835	2409.5426	992.97517	5.6651	8.3928
posANEES [-]	2.7548	2.461	4296972.33765	23752417.4743	5.98014	36.9169
velANEES [-]	1.0465	1.9614	167448.3139	96803.20746	2.31667	16.086
OSPA [-]	<b>2.9865</b>	1.0613	11.0177	0.553821	3.0536	0.75267
GOSPA [-]	<b>280.2572</b>	97.79284	7.3992e+08	4.0809e+09	657.4534	5313.3976
Time [s]	193296.2189		163898.5788		173270.8203	